

IMPEDANCE ISSUES FOR LHC BEAM SCREEN

SERGEY S. KURENNOY

*University of Maryland, Physics Department,
College Park, MD 20742, USA*

(Received 24 January 1995; in final form 24 January 1995)

Designs of modern high-energy superconducting colliders anticipate a beam screen (liner) inside the vacuum chamber to screen cold chamber walls from synchrotron radiation. Pumping holes in the liner walls are required to keep high vacuum inside the beam pipe and provide for a long beam lifetime. The holes are the chamber discontinuities, and electromagnetic fields diffracted by them effect beam stability. This beam-chamber interaction can be described in terms of the coupling impedances. The impedances should be minimized to have a large enough stability safety margin and to allow for a future upgrade — for example, higher beam current. A reasonable choice of the hole shape and size, of the number of holes per unit length, and of their distribution pattern has to ensure a compromise between beam stability, on the one hand, and vacuum, mechanical strength and production requirements, on the other hand. The present paper considers the choice of the shape, size and pattern of the pumping holes for the LHC liner for minimizing the coupling impedances while meeting other requirements.

KEY WORDS: Coupling impedance, beam-chamber interaction

1 INTRODUCTION

The Large Hadron Collider (LHC) vacuum chamber design¹ envisages the insertion of a special beam screen (liner) inside the cold vacuum chamber. The liner is to screen the chamber walls from synchrotron radiation and prevent heating and vacuum problems due to photodesorption of residual gas molecules stuck to the cold wall. In the present design the liner has a square transverse cross-section with rounded corners, rotated in such a way that diagonals of the square are in vertical and horizontal directions, providing the greatest possible space for the beam while still fitting inside the bore pipe. The stainless-steel liner walls have a thickness of $t \simeq 1$ mm for resisting distorting forces during magnet quenches, and a thin copper coating of the inner wall surface for slowing down the resistive wall instability. The inner distance between opposite plane walls of the liner is about 36 mm.

To meet vacuum requirements the total pumping area needs to be about 4% of the liner wall surface. This means several hundred pumping holes per metre of liner, amounting to millions of discontinuities — their contribution to the total impedance of the collider can be significant. Of course, there are other types of small discontinuities on the liner (shielded bellows, transitions, etc.), and methods have been developed to calculate their

impedances (see References 2–4), but pumping holes are specific to the liner, and that is why we concentrate on their impedances in this paper.

The main concern in operating high-energy proton colliders is the coupling impedance at low frequencies, below the chamber cutoff: a typical bunch length is several times larger than the chamber radius. However, resonances at higher frequencies can cause multibunch instabilities due to wake fields excited by a bunch-current perturbation reaching following bunches. In Section 2 the results of an analytical theory for the impedances of pumping holes at low frequencies are summarized. These results allow an optimal choice of the shape and positioning of pumping holes. Section 3 deals with the hole impedances near and above the chamber cutoff, where coupling impedances strongly depend on the distribution pattern of the holes along the pipe. Section 4 covers the conclusions to be drawn from this.

2 LOW-FREQUENCY IMPEDANCE

An analytical calculation of the longitudinal and transverse coupling impedance of small holes in the perfectly conducting walls of the vacuum chamber at low frequencies has been carried out in Reference 5 for an arbitrarily shaped hole in the chamber with a circular cross-section, using the Bethe theory of diffraction by small holes and an expansion over waveguide eigenmodes. Reference 6 gives an alternative derivation, and it also includes the effects of wall thickness for a circular hole. In these references the impedance is expressed in terms of hole polarizabilities, which are purely geometrical factors at low frequencies and can be found by solving a corresponding electro- or magnetostatic problem — as in Reference 7, for example. The longitudinal impedance of a hole in the chamber with the circular cross-section of radius b is inductive:

$$Z(\omega) = -i Z_0 \frac{\omega}{c} \frac{(\alpha_m + \alpha_e)}{4\pi^2 b^2}, \quad (1)$$

where $Z_0 = 120 \pi \Omega$, and α_e and α_m are, respectively, electric and magnetic polarizabilities of the hole. The transverse impedance of the hole is

$$\vec{Z}_\perp(\omega) = -i Z_0 \frac{\alpha_m + \alpha_e}{\pi^2 b^4} \vec{a}_h \cos(\varphi_h - \varphi_b), \quad (2)$$

where \vec{a}_h is the unit vector directed to the hole in the chamber transverse cross-section containing the hole, and φ_h and φ_b are azimuthal angles of the hole and beam in this cross-section. It is worth noting that both the longitudinal and transverse impedances are proportional to the sum of polarizabilities, $(\alpha_m + \alpha_e) > 0$.*

A generalization⁸ of this approach for an arbitrary chamber cross-section S shows that for any chamber the only dependence of the hole coupling impedance on the hole shape is through the same combination of polarizabilities. The longitudinal impedance of the hole is

$$Z(\omega) = -i Z_0 \frac{\omega}{c} (\alpha_m + \alpha_e) e_v^2(0), \quad (3)$$

*In fact, there is rather a difference because α_e and α_m have opposite signs.

where $e_v(\vec{r})$ is merely a normalized electric field produced on the hole by the beam with transverse offset \vec{r} . In other words, $e_v(\vec{r})$ is a solution of the standard two-dimensional electrostatic problem in S : to find the electric field on a conducting boundary produced by a charge which is placed at point \vec{r} . In general, it is expressed analytically in terms of eigenvalues and eigenfunctions of the 2-D problem (see Reference 8), but for simple cross-sections e_v can be easily found by means of the Gauss theorem. For example, with a circular pipe of radius b one gets $e_v(0) = 1/(2\pi b)$, and Eq. (3) transforms into Eq. (1). Another important case is a chamber with a rectangular cross-section of width v and height h . Let a hole in the side wall ($x = \pm v/2$) be displaced from the horizontal plane of the chamber symmetry, $y = 0$, by distance y , $|y| \leq h/2$. Then

$$Z(\omega) = -iZ_0 \frac{\omega}{c} \frac{(\alpha_m + \alpha_e)}{h^2} \Sigma^2, \quad (4)$$

where function Σ is defined by the fast-converging series

$$\Sigma \equiv \sum_{m=0}^{\infty} \frac{\cos(2m+1)\pi y/h}{\cosh(m+1/2)\pi v/h}.$$

The transverse coupling impedance of a hole in the wall of a chamber with an arbitrary cross-section is⁸

$$\vec{Z}_{\perp}(\omega) = -iZ_0(\alpha_m + \alpha_e)(d_x^2 + d_y^2)\vec{a}_d \cos(\varphi_b - \varphi_d), \quad (5)$$

where x, y are the horizontal and vertical coordinates in the chamber cross-section; $d_x \equiv \partial_x e_v(0)$, $d_y \equiv \partial_y e_v(0)$; $\varphi_b = \varphi_s = \varphi_t$ is the azimuthal angle of the beam position in the cross-section plane; and $\vec{a}_d = \vec{a}_x \cos \varphi_d + \vec{a}_y \sin \varphi_d$ is a unit vector in this plane in direction φ_d , which is given by conditions $\cos \varphi_d = d_x / \sqrt{d_x^2 + d_y^2}$, $\sin \varphi_d = d_y / \sqrt{d_x^2 + d_y^2}$.

In Eq. (5) angle φ_d shows the direction of vector \vec{Z}_{\perp} and, therefore, of the beam-deflecting force. Moreover, the value of Z_{\perp} is maximal when the beam is deflected along this direction and vanishes when the beam offset is perpendicular to it. In the particular case of a circular pipe, $d_x = \cos \varphi_h / (\pi b^2)$ and $d_y = \sin \varphi_h / (\pi b^2)$. As a result, $\varphi_d = \varphi_h$ — i.e., \vec{a}_d coincides with \vec{a}_h , which is the direction to the hole — and Eq. (5) reproduces (2).

For a hole located at point ($x = \pm v/2, y$) in the cross-section of the rectangular chamber, Eq. (5) takes the form

$$\vec{Z}_{\perp}(\omega) = -iZ_0 \frac{\pi^2(\alpha_m + \alpha_e)}{h^4} (\Sigma_x^2 + \Sigma_y^2) \vec{a}_d \cos(\varphi_b - \varphi_d), \quad (6)$$

where $\tan \varphi_d = \Sigma_y / \Sigma_x$, and

$$\Sigma_x \equiv \sum_{m=0}^{\infty} \frac{(2m+1) \cos(2m+1)\pi y/h}{\sinh(2m+1)\pi x/h}; \quad \Sigma_y \equiv \sum_{m=0}^{\infty} \frac{2m \sin 2m\pi y/h}{\cosh 2m\pi x/h}.$$

For a small hole of a given shape, the impedance dependence on the hole position in the chamber cross-section is illustrated in Figure 1, which shows the ratio of the longitudinal

impedance versus the angle φ of the hole location for three different cross-sections of the chamber: square with $v = h = 36$ mm; square 36×36 mm² with rounded corners — the curvature radius of 9 mm is 1/4 of the side length (LHC liner design); and circle of radius of $b = 18$ mm inscribed in these squares. In the last case, of course, the impedance is independent of φ — compare with Eq. (1) — and was chosen as the normalization factor. Taking into account the problem symmetry, only the range $0 \leq \varphi \leq 45^\circ$ — one octant of the cross-section — is shown, with $\varphi = 0$ corresponding to the middle of the square side. The thick point shows the LHC design choice of the hole position. Moving holes to the corner would further reduce the impedance, but would affect the mechanical rigidity of the liner. Results for the rounded square are obtained numerically, by solving the 2-D electrostatic problem with the code POISSON. For the transverse impedance the dependence on the hole position is very similar to that in Figure 1 (compare with Reference 8).

Now let us consider the optimum choice of the hole shape. For a circular hole with radius a in a thin wall, when thickness $t \ll a$, polarizabilities are

$$\alpha_m = 4a^3/3, \quad \alpha_e = -2a^3/3,$$

and Eqs. (1–6) have a very simple form. For the hole in a thick wall, $t \geq a$, the sum $(\alpha_m + \alpha_e) = 2a^3/3$ should be multiplied by a factor of 0.56 (see Reference 6). There are also analytical expressions for polarizabilities of elliptic holes in a thin wall,⁷ and a recent study⁹ gives thickness corrections for this case. Surprisingly, the thickness factor for $(\alpha_m + \alpha_e)$ exhibits only a weak dependence on ellipse eccentricity ε , changing its limiting value for the thick wall from 0.56 for $\varepsilon = 0$ to 0.59 for $\varepsilon = 0.99$.

For a longitudinal slot of length l and width w , $w/l \leq 1$ in a thin wall, useful formulae have been obtained¹⁰ — for a rectangular slot

$$\alpha_m + \alpha_e = w^3(0.1814 - 0.0344 w/l);$$

and for a rounded end slot

$$\alpha_m + \alpha_e = w^3(0.1334 - 0.0500 w/l);$$

substituting of which into Eqs. (1–6) gives the impedances of slots. Figure 2 compares impedances, calculated analytically, for different shapes of pumping holes. Numerical computations¹¹ which include thick-wall effects give a similar picture.

Taking into account the pumping area of holes, one can conclude that elongated elliptical slots are the best choice. Round-ended slots are good also, and they are much easier to produce. However, very long slots are unacceptable in superconducting colliders due to the low mechanical strength of the liner with long slots, and because of their high-frequency impedance (see Section 3).

Due to additivity of the impedances at low frequencies, the analytical results cited above give reliable estimates of the LHC liner total coupling impedances due to pumping holes in this frequency range (up to 6 GHz) — see Table 1. The parameters used for estimates are: 666 rounded-end slots 1.5×6 mm² per metre, and the thickness correction factor 0.6.

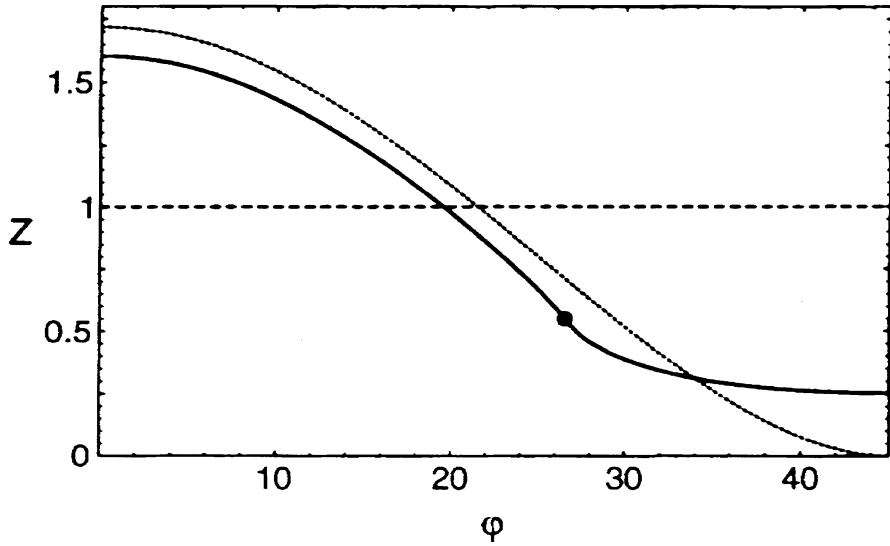


FIGURE 1: Hole impedance (in units of that for circular pipe) versus hole position in the chamber cross section: LHC liner (solid line), square chamber (dotted), circular pipe (dashed).

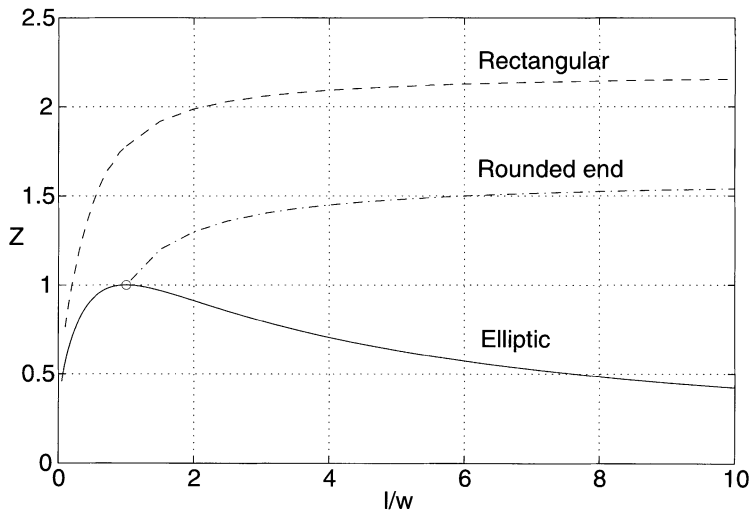


FIGURE 2: Slot impedance versus slot length l for fixed width w in units of the impedance of the circular hole with diameter w .

TABLE 1: Impedances Produced by Liner Pumping Slots.

$ Z/n /\Omega$	$ Z_{\perp} /(\text{M}\Omega/\text{m})$
0.017	0.40

The real part of the hole impedances is proportional to $(\alpha_m^2 + \alpha_e^2)$ and small compared to the reactance in this frequency range (see References 5, 8).

3 HIGH-FREQUENCY IMPEDANCE

3.1 Near cutoff: trapped modes

It has been recently demonstrated¹² that a small discontinuity such as an enlargement or a hole on a smooth waveguide can result in the appearance of trapped electromagnetic modes with frequencies slightly below the waveguide cutoff frequencies. These trapped modes produce narrow resonances of the coupling impedance near the cutoff. This phenomenon for a waveguide with many small discontinuities, which is a good model for the vacuum chamber with a liner, is studied in Reference 13. Using the results from References 12, 13, the resonance impedance of the liner is estimated at near its cutoff frequency.

For the LHC liner there are $M = 8$ slots in one transverse cross-section, and the average longitudinal separation between adjacent cross-sections with the slots is $g = 1.2$ cm. In fact, the longitudinal distribution of the slots will be violated by small random displacements to avoid resonances which would otherwise occur at frequencies well above the cutoff — see Section 3.2. Taking into account that TM modes in the round-ended square liner are quite similar to those in a cylindrical one, we will take for estimates the circular chamber of radius $b = 18$ mm. With respect to the trapped modes, M slots evenly distributed in one cross-section work as a chamber enlargement with ‘effective’ area A in its longitudinal cross-section:¹²

$$A = \frac{M\psi}{4\pi b} = \frac{Mw^2l}{4\pi^2b} = 0.152 \text{ mm}^2 ,$$

where we use transverse magnetic susceptibility $\psi \equiv 2\alpha_m = w^2l/\pi$ for a long narrow slot in the thick wall, for example, see in Reference 10. The length of the region which would be occupied by the field of the trapped mode for such a single discontinuity is $l_1 = b^3/(\mu_1^2 A) = 6.63$ m, where $\mu_1 \simeq 2.405$ is the first root of the Bessel function J_0 . Since this length is much greater than the longitudinal separation between adjacent cross-sections with the pumping slots, discontinuities strongly interact with each other. According to Reference 13, the number of discontinuities, which work as a single combined one, is $N_{\text{eff}} = \sqrt{2l_1/g} \simeq 33$, and the new ‘effective’ length of interaction $L = \sqrt{l_1g/2} = 36$ cm. Then the frequency shift down from the cutoff for the trapped mode is $\Delta f/f_1 = 7 \times 10^{-4}$ — i.e., $\Delta f \simeq 5$ MHz for the cutoff frequency $f_1 \simeq 6.4$ GHz. This gap between the trapped

mode frequency and the cutoff is rather small, but still larger than the resonance width due to the energy dissipation in the walls: $\gamma_1/\omega_1 = \delta/(2b) \simeq 2.3 \times 10^{-5}/\sqrt{RRR}$, where δ is skin depth and RRR is the ratio of the copper conductivities at cryogenic and room temperatures — usually 30–100. The radiation width $\gamma_{\text{rad}}/\omega_1 \propto \psi_{\text{ext}}^2$ (see Reference 12), and is very small, since the external magnetic susceptibility, ψ_{ext} , is exponentially small compared to the internal one, ψ , due to the thick wall — see, for example, Reference 9. Thus the resonance width is small compared to the frequency gap, and the trapped mode exists.

Should discontinuities be far apart, $g > l_1$, the total impedance of the ring will be merely a sum of contributions $R_1 = Z_0 \mu_1^3 A^3 / (\pi \delta b^5)$ from all $N = 2\pi R/g$ discontinuities on the ring (R is the machine radius): $\text{Re } Z/n = NR_1/n = 2\pi b R_1 / (g \mu_1)$. However, since $g \ll l_1$, the interaction of discontinuities must be taken into account. One should consider each group of N_{eff} discontinuities as a single, combined one, with the number of such a group on the ring being $N_g = N/N_{\text{eff}} = \pi R/L$. The estimate then follows from that above with replacements $N \rightarrow N/N_{\text{eff}}$ and $R_1 \rightarrow N_{\text{eff}}^3 R_1$:

$$\frac{\text{Re } Z}{n} = N_{\text{eff}}^2 \frac{2\pi b}{g \mu_1} R_1 = \frac{4Z_0 A^2}{\delta b g^2}. \quad (7)$$

It gives $\text{Re } Z/n \simeq 165 \Omega$ for the narrow-band impedance produced by the trapped modes in the LHC liner ($RRR = 100$ is taken). This value for the narrow-band coupling impedance is too large, even for such a high frequency.

One can improve these estimates, considering that the pumping holes are not quite identical, but they have some distribution of areas (or lengths, for slots), and this causes a frequency spread of resonances produced by different discontinuities. One can take into account the resonance overlapping using a weighted sum in calculating the total impedance of the ring:¹⁴ $Z_{\text{tot}}(\omega) = NZ(\omega) \rightarrow N \int dAw(A)Z(\omega, A)$, where $w(A)$ is the area distribution, $\int dAw(A) = 1$, and $Z(\omega, A)$ is the impedance of a single discontinuity, with area A , at frequencies near the resonance. Referring to Reference 13 for details, we simply cite the result for the case of interacting discontinuities:

$$\frac{\text{Re } Z}{n} \simeq 2\pi Z_0 \frac{w(A)A^2}{bg}, \quad (8)$$

with A being the averaged area per discontinuity. For a specific distribution one should take $\max w(A)$ to get a maximal impedance estimate from (8). Say, for Gaussian distribution of areas with standard deviation σ_A , it is $1/(\sqrt{2\pi}\sigma_A)$. If we assume $\sigma_A/A = 0.1$ and apply Eq. (8) for the LHC liner, it gives $\text{Re } Z/n \simeq 7 \Omega$. This estimate is lower than that from Eq. (7), and it is independent of the wall conductivity.

3.2 Above cutoff

There are two potential sources of impedance resonances due to holes at high frequencies related to the length and distribution of the slots. Resonances with the wavelength $\lambda = 2l$, where l is the slot length, can be moved to higher frequencies by

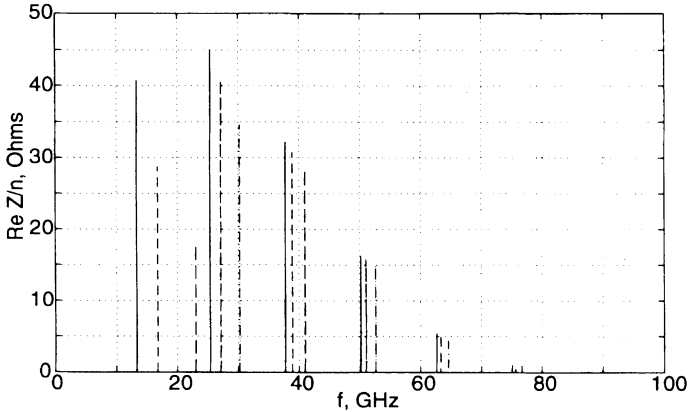


FIGURE 3: Resonances for the exactly periodic distribution of slots.

using relatively short slots. Moreover, a distribution of the slot lengths as considered in Section 3.1 will drastically reduce the strength of these resonances.

Resonances related to the periodicity of the hole distribution along the liner were studied¹⁵ using an analytical model: small axisymmetric enlargements with the triangular cross-section of depth h and base s on the smooth circular chamber of radius b , separated by distance g along the beam. We fix the model parameters ($b = 18$ mm, $g = 12$ mm, $s = 3$ mm, $h = 0.1$ mm) in such a way that this model structure has the same low-frequency impedance and trapped modes as the LHC liner with slots, and we use the model to calculate high-frequency impedances (see formulas and references in Reference 15). An exactly periodic distribution of discontinuities along the liner would give narrow and high resonances, as shown in Figure 3 ($Re Z/n$ in Figure 3 is yet to be multiplied by \sqrt{RRR}).

Fortunately, the slot periodicity is violated by various irregularities of the ring, such as interaction and utility regions. If we also assume an independent positioning of pieces of the liner inside adjacent magnets, it reduces the resonances significantly — down to 2–4 Ω . An additional violation of the slot periodicity inside magnets can further reduce high-frequency resonances, and in the extreme of a ‘random’ hole distribution for the LHC liner, these resonances disappear in the background below 0.1 Ω . In fact, even small ‘random’ longitudinal displacements (say, about 10% of the spacing) of slots from their positions in an exactly periodic array reduce the resonances by the respective orders of magnitude. The numerical comparison of periodic and ‘random’ hole distributions for the SSC liner¹⁶ has shown the advantage of the latter.

4 CONCLUSIONS

There is a good understanding of the low-frequency coupling impedances of pumping holes in liners. The analytical methods are confirmed by simulations and measurements, and give accurate and reliable impedance estimates in this frequency range. They dictate narrow

pumping slots as the best choice. The impedances of pumping slots for the LHC liner design based on them are more than 20 times lower than those for the initial design with circular holes of radius 2 mm (compare with estimates).⁵

The impedance behavior at high frequencies depends on hole distribution patterns. In an optimal design one should avoid exact longitudinal-periodic patterns. An additional small 'randomization' of both the longitudinal distribution of slots and their lengths provides an effective cure against the high-frequency resonances of the coupling impedances.

ACKNOWLEDGEMENTS

The author would like to thank the organizers of the LHC94 workshop for providing an excellent working environment, and the participants for fruitful discussions.

REFERENCES

1. *Design Study of the LHC*, CERN 91-03, Geneva (1991); F. Ruggiero, these proceedings.
2. A.W. Chao, *Physics of Collective Beam Instabilities in High Energy Accelerators* (Wiley, New York, 1993).
3. S. Heifets and S. Kheifets, *Rev. Mod. Phys.*, **63** (1991) 631.
4. S.S. Kurennoy, *Phys. Part. Nucl.*, **24** (1993) 380; also available as CERN SL/91-31(AP), Geneva (1991).
5. S.S. Kurennoy, *Part. Acc.*, **39** (1992) 1.
6. R.L. Gluckstern, *Phys. Rev.*, **A46** (1992) 1106, 1110.
7. R.E. Collin, *Field Theory of Guided Waves* (IEEE, NY, 1991).
8. S.S. Kurennoy, *Proceed. of EPAC* (Berlin, 1992) 871; more details in IHEP 92-84, Protvino (1992).
9. B. Radak and R.L. Gluckstern, *IEEE Trans. MTT*, **43** (1995) 194.
10. S.S. Kurennoy, Report SSCL-636, Dallas (1993).
11. K.L.F. Bane and C.-K. Ng, *Proceed. of PAC* (Washington, 1993) 3432.
12. G.V. Stupakov and S.S. Kurennoy, *Phys. Rev.* **E49** (1994) 794.
13. S.S. Kurennoy, Preprint UMD DSAT 95-10, College Park (1994); *Phys. Rev. E*, in press.
14. V.I. Balbekov, Report IHEP 93-55, Protvino (1993).
15. S.S. Kurennoy, *Proceed. of PAC* (Washington, 1993) 3417.
16. W. Chou and T. Barts, *ibid.* 3444.